

Salt Bridges Stabilize the Folded Structure of Barnase

M. Vijayakumar and Huan-Xiang Zhou*

Department of Physics, Drexel University, Philadelphia, Pennsylvania 19104

Received: March 29, 2001; In Final Form: May 19, 2001

Formation of salt bridges entails desolvation, and whether they stabilize protein structures is an open question. In this paper, the role of three Arg–Asp salt bridges in barnase was studied by extensive continuum-electrostatics calculations. Twelve mutations of the salt bridges were built on the X-ray structure of barnase. The electrostatic component, $\Delta\Delta G_{el}$, of the mutations' effects on the folding stability was found to make the protein less stable by 0.5–5.4 kcal/mol. These agreed well with experimental results of Fersht and co-workers for the mutations' overall effects, $\Delta\Delta G$, on the folding stability (RMS deviation = 1.0 kcal/mol). The coupling energy for the Arg69–Asp93 salt bridge, -3.2 kcal/mol, was reproduced. Apparently, the three salt bridges stabilize the structure of barnase because the electrostatic interactions involving the ionic partners overcome the desolvating costs. We suggest that earlier work of Tidor and co-workers indicating a destabilizing role for salt bridges is based on a protocol that significantly overestimates desolvation costs. That protocol also tends to give unreasonably large coupling energies for salt bridges and predicts a -7.7 kcal/mol coupling energy for the Arg69–Asp93 salt bridge.

Introduction

Recent continuum-electrostatics studies by Tidor and others^{1–3} have indicated that salt bridges may destabilize protein structures. The argument is that there is a high cost for desolvating the two ionic partners of a salt bridge when they are brought from the solvent to the protein environment in the folding process. On the other hand, experiments on various proteins^{4–8} show that the folding stability is decreased when salt bridges are replaced by neutral pairs. On the outset, one cannot unequivocally subscribe the origin of the apparent stabilization by the salt bridges to the electrostatic interactions involving their ionic partners, since the mutations may also have perturbed other factors, such as protein conformation, packing, and hydrophobic interactions. This paper aims to isolate electrostatic effects when salt bridges are replaced by neutral pairs and address the question of whether or how much of the apparent stabilization by three salt bridges of barnase has an electrostatic origin.

Our tool is continuum electrostatics. The three salt bridges of barnase were chosen because they had been subjected to systematic experimental studies by Fersht and co-workers.^{7,9} The plan is to compare continuum-electrostatic predictions directly with experimental results on the differences in folding stability between wild-type barnase and 12 mutants on the three salt bridges. We minimized perturbations other than the change in charges when an ionic residue was replaced by a neutral one. Charge and radius parameters were taken from well-known force fields without adjustments. Of critical importance is how the boundary between the protein dielectric and the solvent dielectric is defined. The choice for the boundary in two widely used software packages^{10,11} is the solvent-exclusion (SE) surface (consisting of contact and reentrant parts,¹² sometimes referred to as the molecular surface). In earlier work,^{13,14} we have used the van der Waals (vdW) surface of the protein as the dielectric boundary. Here the two different choices were compared and tested against experimental results.

Of the two choices for the dielectric boundary, the SE surface leads to significantly lower solvent exposure for the ionic side chains and, consequently, a much higher desolvation cost for forming a salt bridge. At the same time, as the salt bridge is formed in a much less solvated environment, the coupling energy (measuring the strength of electrostatic interaction between the ionic partners) is much higher than the prediction by the vdW surface. We found that the measured decreases in folding stability by the 12 mutations on the three salt bridges of barnase can be reproduced quite well by the calculated electrostatic contributions if the vdW surface is used as the dielectric boundary. Furthermore, the vdW surface yielded a coupling energy for a salt bridge that agrees with the experimental result, but the SE surface gave a value that is higher by 2.4-fold.

It should be noted that modeling of protein electrostatic interactions by continuum electrostatics is phenomenological and approximate. The model contains undefined parameters such as the partial charges and radii of protein atoms and the protein dielectric constant ϵ_p , as well as the undetermined choice for the dielectric boundary. In this work, we did not attempt to study the dependence on the parameters. Rather, we focus on the choice of the dielectric boundary. A priori, there is no "preferred" choice for the dielectric boundary. Ultimately, the justification for a particular choice must be based on the fact the experimental results are reproduced well.

While our continuum-dielectric results are based on detailed protein shape and atom charge distribution, we first would like to present a qualitative understanding of the electrostatic contribution of a salt bridge to the folding stability based on a simple model shown in Figure 1. Here the ionic partners are represented by a small sphere with a radius of $a = 2.6$ Å, with a point charge $+e$ or $-e$ at the center. They are fully exposed to the solvent in the unfolded state of the protein and have a distance of $d = 3.3$ Å in the folded protein, which is represented by a large sphere with a radius $R = 16$ Å. Suppose that both the ionic and the protein interiors are a low dielectric with a

* Corresponding author. Phone: (215) 895-2716. Fax: (215) 895-5934. E-mail: hxzhou@einstein.drexel.edu.

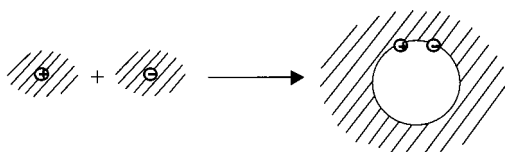


Figure 1. Spherical model for illustrating the formation of a salt bridge upon the folding of a protein. The “+” or “-” sign inside a small circle represents an ion, and the hash represents the solvent dielectric.

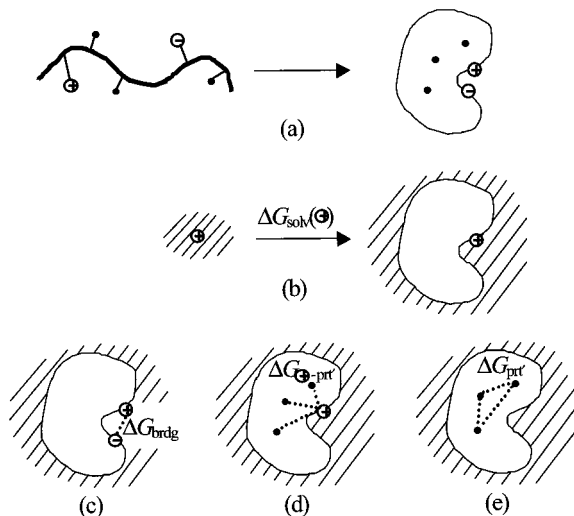


Figure 2. Electrostatic interactions in the folding of a protein. Though in our modeling the ionic partners of a salt bridge have partial charges distributed throughout the D and R residues, for simplicity, we still use a “+” or “-” sign inside a small circle to represent them. The three back dots represent partial charges in other residues of the protein. (a) The folding of the protein. In the unfolded state, the thick black curve represents the backbone; in the folded state, the surface of the protein is represented by a thin closed curve. (b) The desolvation cost for the positive ion. The corresponding quantity for the negative ion is illustrated by the same diagram but with the sign inside the small circle changed to “-” and the circle in the folded state moved to the location of the negative ion. The sum of the two quantities is the desolvation cost ΔG_{solv} for the salt bridge. (c) The free energy arising from the electrostatic interactions of the bridge partners. The dotted line connects the interaction partners. (d) The free energy arising from the electrostatic interactions between the positive ion and the other partial charges in the protein (not including those on the negative ion). An analogous quantity exists for the negative ion. The sum of the two is $\Delta G_{\text{b-prt}}$. (e) The free energy arising from the electrostatic interactions among the partial charges other than those in the salt bridge.

dielectric constant of $\epsilon_p = 4$ and that the solvent has a dielectric constant of $\epsilon_s = 78$. Then in the unfolded state, the solvation energy of the two ions is¹⁵

$$G_{\text{solv}}^{\text{U}} = -\left(\frac{1}{\epsilon_p} - \frac{1}{\epsilon_s}\right)\frac{e^2}{a} = -30.3 \text{ kcal/mol} \quad (1)$$

Operationally, $G_{\text{solv}}^{\text{U}}$ represents the free energy change upon bringing the ions from a low dielectric with dielectric constant ϵ_p to the solvent, while physically, it measures the favorable interaction between the solvent and the ions (see Figure 2). In the folded state, if both ions are fully buried in the protein, with a distance r between the ionic and protein centers ($r \leq R - a$), the solvation energy of the two ions is¹⁶

$$G_{\text{solv}}^{\text{F}} = -\left(\frac{1}{\epsilon_p} - \frac{1}{\epsilon_s}\right)\frac{e^2}{R} \sum_{l=1}^{\infty} \frac{l+1}{l+1 + (\epsilon_p/\epsilon_s)l} \left(\frac{r}{R}\right)^{2l} \quad (2)$$

When the ions are just beneath the protein surface, i.e., $r = R$

– $a = 13.4 \text{ \AA}$, eq 2 gives $G_{\text{solv}}^{\text{F}} = -8.0 \text{ kcal/mol}$. The desolvation cost is then $\Delta G_{\text{solv}} = G_{\text{solv}}^{\text{F}} - G_{\text{solv}}^{\text{U}} = 22.3 \text{ kcal/mol}$. This result shows that the desolvation cost for a fully buried salt bridge is indeed very high and rationalizes the rarity of buried salt bridges in proteins.

When the salt bridge gets more exposed to the solvent, the magnitude of its solvation energy $G_{\text{solv}}^{\text{F}}$ increases rapidly. For the model shown in Figure 1 with both ions centering on the protein surface (i.e., $r = 16 \text{ \AA}$), each ion in the protein environment has only a 45% surface exposure to the solvent, but the solvation energy now becomes $G_{\text{solv}}^{\text{F}} = -24.7 \text{ kcal/mol}$.¹⁷ The desolvation cost is thus reduced to $\Delta G_{\text{solv}} = 5.6 \text{ kcal/mol}$. This will be compensated by the electrostatic interaction between the ionic partners. The energetic contribution of the interaction would be $G_{\text{brdg,coul}} = -e^2/\epsilon_p d = -25.2 \text{ kcal/mol}$ if the protein dielectric extended to infinity. The solvent screens the interaction and reduces the strength of the interaction by $G_{\text{brdg,solv}} = 17.9 \text{ kcal/mol}$. The electrostatic interaction between the ionic partners in the protein environment thus gives rise to a free energy $G_{\text{brdg}} = G_{\text{brdg,coul}} + G_{\text{brdg,solv}} = -7.3 \text{ kcal/mol}$ (see Figure 2). The net contribution of the salt bridge to the folding stability of the protein is $\Delta \Delta G_{\text{el}} = \Delta G_{\text{solv}} + G_{\text{brdg}} = -1.7 \text{ kcal/mol}$. In short, the calculation based on the model of Figure 1 shows that a salt bridge that is 55% buried will by itself contribute 1.7 kcal/mol to the folding stability of the protein. This contribution increases as the salt bridge gets further exposed. In addition, the salt bridge can further stabilize the protein structure by favorable interactions with the rest of the protein (see Figure 2).¹⁸

In this paper, we calculated the electrostatic component, $\Delta \Delta G_{\text{el}}$, of the effects of 12 barnase mutations on the folding stability of the protein. In these mutations, one or both ionic partners of the Arg69–Asp93, Arg83–Asp75, and Arg110–Asp12 salt bridges were replaced. Their overall effects, $\Delta \Delta G$, on the folding stability have been measured by Fersht and co-workers.^{7,9} We directly compared $\Delta \Delta G_{\text{el}}(\text{calc})$ against $\Delta \Delta G(\text{expt})$, which necessarily involves nonelectrostatic effects such as those due to conformational changes and hydrophobic interactions. Using the vdW surface as the dielectric boundary, we found $\Delta \Delta G_{\text{el}}(\text{calc})$ to agree with $\Delta \Delta G(\text{expt})$ quite well. The root-mean-square (RMS) deviation was 1.0 kcal/mol, relative to a range of $\Delta \Delta G_{\text{el}}(\text{calc})$ from 0.5 to 5.4 kcal/mol. This suggests that for these mutations, electrostatic effects are dominant.

The most reliable measurement of electrostatic effects is that on the interaction between the ionic partners of a salt bridge, made through a double-mutant cycle.¹⁹ The resulting coupling energy, $\Delta \Delta G_{\text{int}}$, for a salt bridge thus provides the best test on electrostatic calculations. For the Arg69–Asp93 salt bridge, $\Delta \Delta G_{\text{int}}$ was measured to be -3.2 kcal/mol by Fersht and co-workers.⁷ Using the vdW surface as the dielectric boundary, we found $G_{\text{int}} = -3.1 \text{ kcal/mol}$. In contrast, $G_{\text{int}} = -7.7 \text{ kcal/mol}$ when the SE surface was used.

Methods

Generation of Mutant Structures. The locations of the three salt bridges studied are shown in Figure 3. The structures of the 12 mutants were built on the X-ray structure of wild-type (wt) barnase,²⁰ to which all hydrogen atoms were added by using the program InsightII (Molecular Simulations, Inc.). To allow for maximal cancellation of numerical errors, each mutant structure had minimal difference from the wt one. Specifically, when a side chain was replaced, only atoms beyond C_{β} were allowed to optimize their positions by energy minimization. The AMBER force field²¹ was used for the minimization.

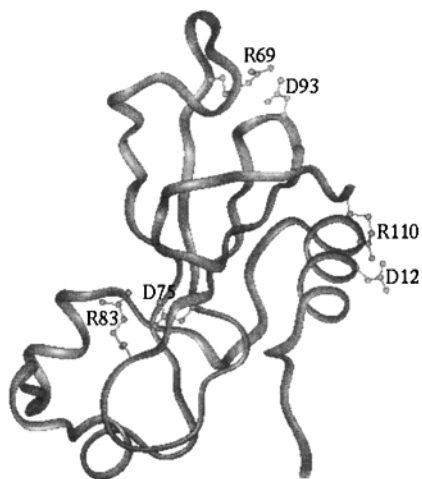


Figure 3. Locations of the three salt bridges in barnase.

Electrostatic Model. The electrostatic model for our calculations is a generalization of the one shown in Figure 1 and is illustrated in Figure 2. First, each protein atom, in addition to those forming the salt bridge, was assigned a partial charge. These charges added up to $-e$ for Asp and Glu residues and the C terminal and $+e$ for Arg and Lys residues and the N terminal. All other residues had a zero net charge. The total charge of wt barnase was $+2e$. Second, the dielectric boundary between the protein and the solvent was determined by the vdW radii of the protein atoms. A main conclusion of the paper is that the vdW surface of the protein should be used for the boundary (as opposed to the conventionally used SE surface). The latter surface consists of contact and re-entrant parts as defined by a 1.4 \AA solvent probe.¹² Finally, the screening effect of mobile salt ions in the solvent was taken into consideration by using the linearized Poisson–Boltzmann equation. The screening was turned on 2 \AA away from the protein vdW surface. The gap was equivalent to the radius of a salt ion. All calculations were done at an ionic strength of $I = 100 \text{ mM}$.

Electrostatic Component of Folding Free Energy and Effect of Mutation. Given a protein structure and its atomic charges (q_i) and radii, the electrostatic free energy, G_{el}^{F} , was obtained by numerically solving for the electrostatic potential ϕ_i at the locations of the atoms. One has

$$G_{\text{el}}^{\text{F}} = \frac{1}{2} \sum_i q_i \phi_i \quad (3)$$

in which the infinite self-energy of each charge is excluded. A similar calculation was needed for the unfolded state, and the resulting electrostatic free energy, G_{el}^{U} , had to be obtained. The electrostatic component, ΔG_{el} , of the folding free energy is then given by $G_{\text{el}}^{\text{F}} - G_{\text{el}}^{\text{U}}$.

Our focus is on the change, $\Delta \Delta G_{\text{el}}$, brought by a single or double mutation. In practice, we assumed in the unfolded state that (1) the electrostatic free energy of the rest of the protein [i.e., other than the residue(s) to be mutated] is identical in the wt and the mutant and (2) the free energy arising from the electrostatic interactions between the residue(s) to be mutated and the rest of the protein is either zero or not affected or by the mutation. Then for the unfolded state, we only had to be concerned with the electrostatic free energies of the residue(s) to be mutated and its (their) replacement(s). To allow for maximal error cancellation, we assumed that these residues in the unfolded state adopted the same conformations as they did in the folded state (see an exception below). Furthermore, these

residues were assumed to be individually solvated.²² We also tested a slightly different model for the unfolded state in which only the side chain of a mutated residue was “carved” out from the folded protein structure and put in the solvent.

In the case of Arg110, the C-terminal residue, it is likely that the close proximity between the side chain and the C terminal will allow them to interact in the unfolded state. There is experimental evidence that indicates residual interactions involving carboxyl groups of barnase.²³ We therefore modeled the C-terminal Arg110 in the unfolded state as forming a salt bridge between the side chain and the terminal carboxyl ($N_{\epsilon}-O$ and $N_{\gamma 2}-O$ distances were 2.8 and 2.9 \AA , respectively).

Desolvation Cost and Coupling Energy. To obtain the desolvation cost for bringing the ionic partners of a salt bridge into the protein environment, we calculated the electrostatic free energies of the ionic partners individually in the protein environment by keeping the partial charges of one partner while removing the charges of the other partner and the rest of the protein (see Figure 2). The sum of the corresponding free energies in the unfolded state is G_{el}^{U} . The difference between the sum of the free energies for the two partners in the protein environment and G_{el}^{U} constitutes the desolvation cost ΔG_{solv} . Our main concern is the change in the desolvation cost, $\Delta \Delta G_{\text{solv}}(R \rightarrow X, D \rightarrow Y)$, when the ionic partners, R and D, are mutated into some other residues, X and Y.

The coupling energy for a salt bridge, as obtained from a double-mutant cycle, is given by

$$\Delta \Delta G_{\text{int}} = \Delta \Delta G(R \rightarrow X, D \rightarrow Y) - \Delta \Delta G(R \rightarrow X) - \Delta \Delta G(D \rightarrow Y) \quad (4)$$

where $\Delta \Delta G(R \rightarrow X, D \rightarrow Y)$, $\Delta \Delta G(R \rightarrow X)$, and $\Delta \Delta G(D \rightarrow Y)$ are the changes in the folding free energy brought by the double mutation and the two single mutations. We predicted $\Delta \Delta G_{\text{int}}$ by using in eq 4 the electrostatic components of the mutational changes in the folding free energy.

The electrostatic component ΔG_{el} of the folding free energy can be decomposed into four terms: ΔG_{solv} , the desolvation cost; G_{brdg} , the free energy arising from the electrostatic interaction between the bridge partners; $G_{\text{b-prt}}$, the free energy arising from the electrostatic interactions of the bridge partners with the rest of the protein; and G_{prt} , the electrostatic free energy of the rest of the protein (see Figure 2). In the simple situation where a mutation amounts to merely an adjustment of the partial charges of a residue (i.e., the dielectric boundary is preserved), one has $\Delta \Delta G_{\text{solv}}(R \rightarrow X, D \rightarrow Y) = \Delta \Delta G_{\text{solv}}(R \rightarrow X) + \Delta \Delta G_{\text{solv}}(D \rightarrow Y)$, $\Delta G_{\text{b-prt}}(R \rightarrow X, D \rightarrow Y) = \Delta G_{\text{b-prt}}(R \rightarrow X) + \Delta G_{\text{b-prt}}(D \rightarrow Y)$, and $\Delta G_{\text{prt}}(R \rightarrow X, D \rightarrow Y) = \Delta G_{\text{prt}}(R \rightarrow X) = \Delta G_{\text{prt}}(D \rightarrow Y) = 0$. Then

$$\Delta \Delta G_{\text{int}} = \Delta G_{\text{brdg}}(R \rightarrow X, D \rightarrow Y) - \Delta G_{\text{brdg}}(R \rightarrow X) - \Delta G_{\text{brdg}}(D \rightarrow Y) = G_{\text{brdg}}(R-D) + G_{\text{brdg}}(X-Y) - G_{\text{brdg}}(R-Y) - G_{\text{brdg}}(X-D) \quad (5)$$

where $G_{\text{brdg}}(A-B)$ denotes the free energy arising from the electrostatic interaction between A and B in the protein environment. This was calculated via $G_{\text{brdg}}(A-B) = \sum_B q_i \phi_i(A)$, where the sum is over the partial charges of B and the electrostatic potential is due to the partial charges of A. In general, eq 5 represents the major portion of the coupling energy $\Delta \Delta G_{\text{int}}$. A small difference between eqs 4 and 5 may exist since the dielectric boundary is slightly perturbed by the mutations.

The contribution of an R–D salt bridge itself to the folding stability can be assessed by assuming that the rest of the protein

TABLE 1: Changes in the Electrostatic Component of the Folding Free Energy of Barnase by Charge Mutations (in units of kcal/mol)

mutation	$\Delta\Delta G(\text{expt})$	$\Delta\Delta G_{\text{el}}(\text{calc})$				
		Amber		Charmm		
		vdW&residue ^a	SE&residue	vdW&residue	vdW&side chain	SE&side chain
R69S	2.67	1.67	2.29	0.13	0.20	1.49
D93N	4.17	4.35	6.58	4.34	5.49	9.94
R69S/D93N	3.62	2.89	2.04	1.71	3.43	3.73
R69K	3.11	1.88	4.95	0.82	0.84	5.80
R69M	2.24	2.11	1.99	0.70	0.58	0.85
R83K	3.86	1.10	1.17	1.82	1.88	0.68
R83Q	2.23	2.36	1.92	1.12	1.14	0.40
D75N	4.51	4.62	5.87	4.16	5.19	8.78
R83K/D75N	5.19	5.38	5.74	5.26	6.48	6.80
R110A	0.45	1.48	1.92	-0.04	1.12	-0.78
D12A	0.95 ^b	1.25	1.15	0.23	0.75	0.80
R110A/D12A	0.20 ^b	0.51	-0.06	-1.18	0.50	-2.50
RMS dev		1.0	1.4	1.5	1.4	2.7

^a In this row, vdW (or SE) means that the vdW (or SE) surface is used as the dielectric boundary, and residue (or side chain) means that the whole residue (or just the side chain) is used as a model for the unfolded state. For the last column, the protocol is the same as what was used by Hendsch and Tidor.¹ ^b Corrected for the difference in helix-forming propensity between D12 and A12 (which occur in the middle of an α -helix in the folded protein) according to Spek et al.⁸

is totally discharged. Relative to the X–Y background, this contribution is $-\Delta\Delta G_{\text{solv}}(\text{R}\rightarrow\text{X},\text{D}\rightarrow\text{Y}) - \Delta\Delta G_{\text{brdg}}(\text{R}\rightarrow\text{X},\text{D}\rightarrow\text{Y})$.

Protocol for Numerical Solution. The Poisson–Boltzmann equation was solved by the finite-difference method using the UHBD program.¹¹ The SE surface was selected as the dielectric boundary by using the “nmap 1.5, nsph 500” option, whereas the vdW surface was selected without this option. The electrostatic potential was calculated first by using a $100 \times 100 \times 100$ grid with a 1.5 Å spacing centered at the geometric center of wt barnase. This was followed by a $140 \times 140 \times 140$ grid with a 0.5 Å spacing at the same center. A final round of focusing at the backbone N atom of a bridge partner was implemented by using a $60 \times 60 \times 60$ grid with a 0.25 Å spacing. To minimize numerical errors due to distributing charges onto grid points, we calculated G_{el}^{F} was calculated as $G_{\text{el}}^{\text{F}}(\epsilon_{\text{s}} = 78, I = 100 \text{ mM}) - G_{\text{el}}^{\text{F}}(\epsilon_{\text{s}} = 4, I = 0) + \sum_{ij} q_i q_j / \epsilon_{\text{p}} r_{ij}$. The same protocol was used for the unfolded state.

Atomic Charges and Radii. Two sets of charge-radius parameters were used. The first, involving all hydrogens, has Amber charges²¹ and OPLS radii.²⁴ The second set, involving only polar hydrogens, has Charmm charges and radii.²⁵ A particular difference between the two parameter sets lies in the radii of hydrogen atoms. These had a uniform value of 1.2 Å in the former set but were 0.6 or 0.8 Å in the latter set. We included the Charmm parameter set in the present study mainly because this is what was used by Hendsch and Tidor.¹

In the Charmm parameter set, the partial charges of the side chains summed up to zero or whole charges, so it was possible to use side chains only (as opposed to whole residues) as a model for the unfolded state.

Percentage of Surface Burial of Ionic Side Chains. A simple measure of the solvent exposure of an ionic side chain is given by the difference in the group’s exposed surface in the protein environment and that in the solvent. In calculating the latter, S^{U} , we carved out the whole residue and put that in the solvent. The percentage burial was $(1 - S^{\text{F}}/S^{\text{U}}) \times 100\%$. The surface was either the vdW surface or the SE surface, defined by the OPLS radii. The areas were calculated using the GEPOL93 program.²⁶

Results

Effects of Charge Mutations on Folding Stability of Barnase. Table 1 lists the calculated effects of 12 charge

mutations on the electrostatic component of the folding stability of barnase. Five sets of calculations were made. In two of these, the Amber charges and OPLS radii were used, whereas in the other three, the Charmm charges and radii were used. Either the vdW or the SE surface was used as the dielectric boundary. The overall performance of these calculations is indicated by the RMS deviation from the experimental results of Fersht and co-workers.^{7,9} The calculation with the Amber charge and the vdW surface has the best performance, with an RMS deviation of 1.0 kcal/mol. Using the SE surface always increases the deviation from experiment. This increase is especially significant for the calculation with the Charmm charges and radii. The results of the calculations using either the whole residue or just the side chain as a model for the unfolded state are similar.

In Figure 4, we show the correlations between the experimental free energy difference $\Delta\Delta G(\text{expt})$ and the electrostatic free energy difference $\Delta\Delta G_{\text{el}}(\text{calc})$ calculated by three protocols: vdW and SE surfaces with Amber parameters and SE surface with Charmm parameters. The last is the protocol used by Hendsch and Tidor.¹ The correlation coefficient between $\Delta\Delta G(\text{expt})$ and $\Delta\Delta G_{\text{el}}(\text{calc})$ by Amber+vdW is 0.80, and the slope of the correlation is 0.8. The correlation coefficient decreases to 0.75 for $\Delta\Delta G_{\text{el}}(\text{calc})$ by Amber+SE (with the slope of the correlation at 1.0). For Charmm+SE, even though the correlation coefficient, at 0.82, is quite reasonable, the slope of the correlation is 2.0 and thus too high. The continuum electrostatics model is justified on the basis of the assumption that the calculated electrostatic energy is a component of the folding free energy. As such, one expects a slope of correlation around 1.

Coupling Energy for Salt Bridge in Barnase. The experimental value of $\Delta\Delta G_{\text{int}}$ for the R69–D93 salt bridge, -3.22 kcal/mol, is reproduced by the Amber+vdW calculation [$\Delta\Delta G_{\text{int}}(\text{calc}) = -3.13$ kcal/mol]. The two Charmm+vdW calculations underestimate $\Delta\Delta G_{\text{int}}$ by 0.5–1.0 kcal/mol [$\Delta\Delta G_{\text{int}}(\text{calc}) = -2.76$ kcal/mol for a whole-residue model of the unfolded state and -2.26 kcal/mol for a side-chain model]. In contrast, both SE calculations severely overestimate the coupling energy. The Amber+SE calculation gives $\Delta\Delta G_{\text{int}} = -6.83$ kcal/mol, whereas the Charmm+SE calculation gives $\Delta\Delta G_{\text{int}} = -7.70$ kcal/mol.

The interaction between the partners of the R69–D93 salt bridge was further investigated by the Amber+vdW calculation.

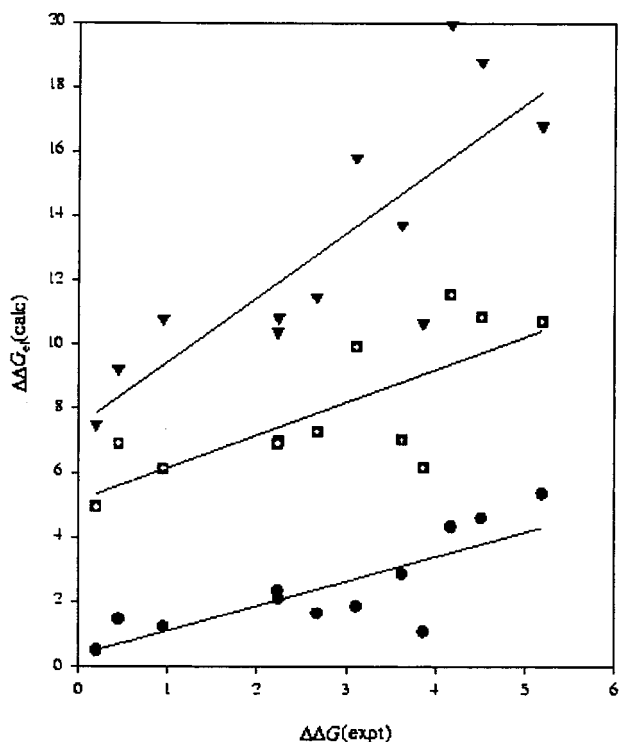


Figure 4. Correlations of calculated and experimental changes in folding free energy. The circles, squares, and triangles represent calculated results by the Amber+vdW, Amber+SE, and Charmm+SE protocols, respectively. For clarity, the calculated results for the latter two protocols were shifted upward by 5 and 10 kcal/mol, respectively.

The interaction amounted to an free energy of $G_{\text{brdg}}(\text{R}-\text{D}) = -4.54$ kcal/mol. In the double mutant S69–N93, the interaction energy diminished to $G_{\text{brdg}}(\text{S}-\text{N}) = -0.02$ kcal/mol. In the two single mutants S69 and N93, the interactions with the remaining partner gave rise to $G_{\text{brdg}}(\text{S}-\text{D}) = 0.1$ kcal/mol and $G_{\text{brdg}}(\text{R}-\text{N}) = -1.34$ kcal/mol. According to eq 5, the coupling energy for the R69–D93 bridge would be $\Delta\Delta G_{\text{int}} = -3.32$ kcal/mol. The close agreement with the result of -3.13 kcal/mol calculated using eq 4 confirms that eq 5 represents the major portion of the coupling energy.

The experimental value of the coupling energy for the R83–D75 salt bridge is complicated by the fact that the double-mutant cycle used by Fersht and co-workers involved replacing R83 by K, a residue with the same charge. From a purely electrostatic point of view, one expects such a double-mutant cycle to yield a small coupling energy. This is indeed the result from the three vdW calculations ($\Delta\Delta G_{\text{int}} = -0.34, -0.72, \text{ and } -0.59$ kcal/mol). The two SE calculations gave a higher coupling energy (-1.30 and -2.66 kcal/mol), mainly due to overestimating the destabilizing effect of the D75 \rightarrow N single mutation. We attribute the coupling energy of -3.18 kcal/mol obtained by the particular measurement of Fersht and co-workers to a nonelectrostatic origin. This view is supported by the fact that they found the R83 \rightarrow K mutation to result in a larger decrease in the folding free energy than a mutation to Q. Using Q and N as substitutes of R83 and D75, respectively, we predicted the coupling energy to be -4.52 kcal/mol by the Amber+vdW calculation.

The experimental coupling energy for the R110–D12 salt bridge, -1.20 kcal/mol, is reasonably reproduced by the three vdW calculations ($\Delta\Delta G_{\text{int}} = -2.22, -1.37, -1.37$ kcal/mol). The two SE calculations give higher estimates ($\Delta\Delta G_{\text{int}} = -3.13$ and -2.52 kcal/mol).

Desolvation Cost. The overestimate of $\Delta\Delta G_{\text{int}}$ by the SE calculations is accompanied by a high desolvation cost. Relative to the S69–N93 background, the Amber+SE and Charmm+SE calculations predict desolvation costs of 8.23 and 10.4 kcal/mol for the R69–D93 salt bridge. In contrast, the Amber+vdW calculation predicts a desolvation cost of merely 2.86 kcal/mol.

If the rest of the protein is totally discharged, the Amber+vdW calculation predicts that the R69–D93 salt bridge, relative to the S69–N93 background, stabilizes the protein by $|\Delta\Delta G_{\text{solv}}(\text{R}\rightarrow\text{X},\text{D}\rightarrow\text{Y}) + \Delta\Delta G_{\text{brdg}}(\text{R}\rightarrow\text{X},\text{D}\rightarrow\text{Y})| = 1.66$ kcal/mol. According to the two SE calculations, this salt bridge either marginally stabilizes or actually destabilizes the protein structure [$-\Delta\Delta G_{\text{solv}}(\text{R}\rightarrow\text{X},\text{D}\rightarrow\text{Y}) - \Delta\Delta G_{\text{brdg}}(\text{R}\rightarrow\text{X},\text{D}\rightarrow\text{Y}) = -0.22$ and $+1.37$ kcal/mol].

Percentage of Surface Burial of Ionic Side Chains. The difference in calculated desolvation costs between using vdW and SE surfaces parallels the difference in surface burial percentages of the ionic side chains. In terms of the vdW surface, Arg69, Arg83, and Arg110 had 15%, 7%, and 12% of their side chains buried by the protein, while Asp93, Asp75, and Asp12 had 17%, 15%, and 9% of their side chains buried. In contrast, in terms of the SE surface, Arg69, Arg83, and Arg110 had 87%, 75%, and 65% of their side chains buried by the protein, while Asp93, Asp75, and Asp12 had 52%, 100%, and 33% of their side chains buried.

Discussion

Use of vdW Surface in Continuum-Electrostatics Calculations. We have studied the effects of 12 charge mutations on the folding stability of barnase by continuum-electrostatics calculations and directly compared them with the experimental results of Fersht and co-workers. By using the vdW surface of the protein as the dielectric boundary, we found good overall agreement between calculated and experimental changes of the folding free energy by the charge mutations. In addition, we reproduced the experimental coupling energy for a salt bridge, which is least likely to be contaminated by nonelectrostatic effects and thus provides the most reliable measurement of electrostatic effects. If the SE surface is used as the dielectric boundary, the overall deviation of calculation from experiment increases significantly, and the coupling energy is overestimated severely. We thus raise the contention that the common practice of using the SE surface should be changed to that of using the vdW surface.

The coupling energies for salt bridges have predominantly an electrostatic origin and have been measured on various proteins^{4–8,27} to be in the range of -1 to -5 kcal/mol. The coupling energies calculated using the vdW surface for the three salt bridges of barnase are all within this range. On the other hand, the coupling energy calculated using the SE surface for the R69–D93 salt bridge has a significantly larger magnitude. In the work of Hendsch and Tidor in which 21 salt bridges from nine proteins were studied using the SE surface, eight had coupling energies with magnitudes greater than 6 kcal/mol, and the three highest magnitudes were even above 10 kcal/mol.

It is very relevant to note that the use of the SE surface in continuum-electrostatics calculations has already run into problem in the context of pK_a predictions. We found in the present study that the SE surface gives rise to substantial overestimate of the interaction energy between ions. The overestimate would lead to overly perturbed pK_a values (relative to those of model compounds), and indeed this is what happens. To counter the over perturbation of predicted pK_a values, Gilson et al.²⁸ had to artificially weaken the interaction between ions

by using a high value of 20 for the protein dielectric constant. The use of the vdW surface should alleviate this problem. In this context, we note that there is some evidence indicating that a more physical dielectric constant of 4 for the protein can be used in pK_a calculations when sampling of side chain rotamer conformations is allowed for.²⁹ We thus caution that the use of the vdW surface should not be considered as the only “fix” for making continuum electrostatics an accurate modeling tool.

From a molecular point of view, it may be argued that the vdW surface represents a better picture of protein solvation than the SE surface. According to the vdW surface, the side chains of the three salt bridges in barnase have 9–17% burial. The burial is 33–100% if the SE surface is used. Hydrogen exchange experiments demonstrate that different parts of a folded protein are highly accessible to the solvent. Perhaps such solvent exposure is better modeled by the low burial of the vdW surface. Molecular dynamics simulations of water molecules around ions show that the hydrogen and oxygen atoms of a water molecule can penetrate the vdW surface of an ion.³⁰ This suggests that, in reality, the crevice between two protein atoms with overlapping vdW spheres will be accessed by water molecules.

The desolvation cost for forming a salt bridge calculated by using the vdW surface as the dielectric boundary is lower than that calculated using the SE surface by several fold. The reduced desolvation cost may reverse the role of the salt bridge from a destabilizing one to a stabilizing one. This is the case for the R69–D93 salt bridge in barnase when the interactions with the rest of protein are not considered.

Proper Measure of Energetic Contribution of Salt Bridge.

There appear to be three different measures of the energetic contribution of a salt bridge. The first is provided by $-\Delta\Delta G_{el}(R\rightarrow X, D\rightarrow Y)$, the difference in the electrostatic component of the folding free energy between a protein with an R–D salt bridge and the variant with an X–Y neutral pair. The second is given by the coupling energy $\Delta\Delta G_{int}$. The third is $-\Delta\Delta G_{solv}(R\rightarrow X, D\rightarrow Y) - \Delta\Delta G_{brdg}(R\rightarrow X, D\rightarrow Y)$, the contribution of the salt bridge to the folding stability if the rest of the protein is totally discharged. As far as the folding stability of a protein is concerned, we suggest using $-\Delta\Delta G_{el}(R\rightarrow X, D\rightarrow Y)$ as the measure. One drawback with $\Delta\Delta G_{int}$ is that it may to a large extent be offset by the desolvation cost for forming the bridge so the net contribution to the folding stability could be small. A problem with $-\Delta\Delta G_{solv}(R\rightarrow X, D\rightarrow Y) - \Delta\Delta G_{brdg}(R\rightarrow X, D\rightarrow Y)$ is that it does not take into consideration the interactions of the bridge partners with the rest of the protein, which often can be quite favorable.¹⁷

The positive values of calculated $\Delta\Delta G_{el}(R\rightarrow X, D\rightarrow Y)$ and experimental $\Delta\Delta G(R\rightarrow X, D\rightarrow Y)$ show an agreement that the three salt bridges all stabilize the folded structure of barnase. Though it is not clear a priori how much of the experimentally measured $\Delta\Delta G(R\rightarrow X, D\rightarrow Y)$ comes from the electrostatic contribution $\Delta\Delta G_{el}(R\rightarrow X, D\rightarrow Y)$, the general agreement between the values of experimental $\Delta\Delta G(R\rightarrow X, D\rightarrow Y)$ and calculated $\Delta\Delta G_{el}(R\rightarrow X, D\rightarrow Y)$ indicates that the stabilization effects of the salt bridges mostly have an electrostatic origin.

Experimental Determination of Salt Bridge’s Electrostatic Contribution. The electrostatic component $\Delta\Delta G_{el}$ of a salt bridge’s contribution to the folding free energy can be isolated experimentally by measuring pK_a shifts.⁴ Consider a salt bridge between R and D in a protein. The pK_a change, $\Delta pK_a(D)$, of D upon protein folding can be calculated via¹³

$$\Delta pK_a(D) = -\frac{1}{k_B T \ln 10} \{ [G_{el}^F(R - D_0) - G_{el}^F(R - D)] - [G_{el}^U(D_0) - G_{el}^U(D)] \} = -\frac{1}{k_B T \ln 10} \Delta\Delta G_{el}(D \rightarrow D_0) \quad (6)$$

where $k_B T$ is the product of Boltzmann’s constant and the absolute temperature, D_0 is the neutral (i.e., protonated) form of D, and $\Delta\Delta G_{el}(D \rightarrow D_0)$ is the change in the electrostatic component of the folding free energy upon “mutating” D to D_0 . Using eq 6 and the Amber+vdW protocol, we found $\Delta pK_a(D) = -3.1$ for D93. This is in good agreement with the measured pK_a value of 0.7 in the folded state,²³ if a value of 4 is assumed for the unfolded state.

A similar expression exists for the pK_a change of D when R is mutated to a neutral residue X. The difference in pK_a change between the R \rightarrow X mutant and wt gives the coupling energy for the salt bridge

$$\Delta\Delta G_{int} = -(k_B T \ln 10) \Delta\Delta pK_a(D) \quad (7)$$

In this definition of the coupling energy, the neutral analogues of R and D are X and D_0 , respectively. By the Amber+vdW protocol, we found that $\Delta pK_a(D)$ for D93 changed from -3.1 to -1.0 when R69 was mutated to S. Thus, $\Delta\Delta G_{int}$ from this estimate is -2.9 kcal/mol, which is close to the calculated result (-3.1 kcal/mol) by the double mutant cycle. Equation 7 suggests another route for experimentally determining the coupling energies of salt bridges. An analogous expression for the coupling energy can be written in terms of the difference in the pK_a changes of R between the D \rightarrow Y mutant and wt.

Fully Buried Salt Bridges. We have emphasized the difference in solvent exposure and desolvation cost between using the vdW and SE surfaces. However, for a truly buried salt bridge, i.e., one that is 100% buried regardless of whether the vdW or the SE surface is used, our calculation based on the model in Figure 1 indicates a destabilizing role. A salt bridge formed between K and the C terminal of a pentapeptide Ac–WLLKLL–COO[−] in octanol, studied recently by Wimpley et al.,³¹ may be viewed as infinitely buried (assuming that octanol has the same dielectric properties as proteins). Using the neutral analogue Ac–WLLSLL–COOH as reference, K and COO[−] were found to favor being separately solvated by water over forming a salt bridge in octanol by 3.03 kcal/mol. This result can be rationalized within the model in Figure 1 with an infinite radius for the protein, which predicts the free energy change on going from K and COO[−] being separately solvated by water to forming a salt bridge in octanol as $G_{brdg, coul} - G_{solv}^U = (-25.2 + 30.3)$, i.e., 5.1 kcal/mol.

Do Salt Bridges Stabilize Protein Structures in General?

In proteins, fully buried salt bridges are rare exceptions. Most salt bridges have solvent exposure similar to that found for the three salt bridges in barnase, i.e., 10–20% burial according to the vdW surface (Vijayakumar & Zhou, unpublished result). The results of the present study lead us to believe that, electrostatically, most of the salt bridges will be stabilizing to the folded protein structures. This is opposite to the conclusion of Tidor and co-workers based on using the SE surface.^{1, 2}

The question of whether the overall effect of a salt bridge relative to a neutral pair is stabilizing cannot be completely addressed by studies like this one or those of Tidor and co-workers that are based on electrostatic calculations alone. The neutral pair may have a more favorable nonelectrostatic contribution (see, e.g., Waldburger et al.²⁷). For the three salt

bridges studied here, we can say that such nonelectrostatic contributions appear to be of less importance than the electrostatic ones.

While our calculations regarding the stabilizing effect of salt bridges based on using the vdW surface contrast sharply with the study of Tidor and co-workers based on using the SE surface, they agree to a large extent with a recent study³² in which free energies were calculated by a combination of molecular dynamics simulations and the generalized Born solvation model. This agreement is heartening since it indicates that electrostatic effects can be understood from complementary approaches.

A Kinetic Role for Salt Bridge? In the case of protein–protein association, it has been well established that the ionic partners of interfacial salt bridges, by the long-range nature of their electrostatic interactions, can enhance the diffusional encounter between two proteins and thus speed up the association process.¹⁴ It is logical to suggest that the ionic partners of a salt bridge may enhance the diffusional encounter between structural elements of a protein and thus speed up the folding process.

Acknowledgment. This work is supported in part by NIH Grant GM58187.

References and Notes

- Hendsch, Z. S.; Tidor, B. *Protein Sci.* **1994**, *3*, 211.
- Sindelar, C. S.; Hendsch, Z. S.; Tidor, B. *Protein Sci.* **1998**, *7*, 1898.
- Barril, X.; Aleman, C.; Orozco, M.; Luque, F. J. *Proteins* **1998**, *32*, 67.
- Anderson, D. E.; Becktel, W. J.; Dahlquist, F. W. *Biochemistry* **1990**, *29*, 2403.
- De Prat Gay, G.; Johnson, C. M.; Fersht, A. R. *Protein Eng.* **1994**, *7*, 103.
- Marqusee, S.; Sauer, R. T. *Protein Sci.* **1994**, *3*, 2217.
- Tissot, A. C.; Vuilleumeier, S.; Fersht, A. R. *Biochemistry* **1996**, *35*, 6786.
- Spek, E. J.; Bui, A. H.; Lu, M.; Kallenbach, N. R. *Protein Sci.* **1998**, *7*, 2431.
- Horovitz, A.; Serrano, L.; Avron, B.; Bycroft, M.; Fersht, A. R. *J. Mol. Biol.* **1990**, *216*, 1031.
- Sharp, K. A.; Honig, B. *Annu. Rev. Biophys. Biophys. Chem.* **1990**, *19*, 301.
- Madura, J. D.; Briggs, J. M.; Wade, R. C.; Davis, M. E.; Luty, B. A.; Ilin, A.; Antosiewicz, J.; Gilson, M. K.; Bagheri, B.; Scott, L. R.; McCammon, J. A. *Comput. Phys. Comm.* **1995**, *91*, 57.
- Richards, F. M. *Annu. Rev. Biophys. Bioeng.* **1977**, *6*, 151.
- Zhou, H.-X.; Vijayakumar, M. *J. Mol. Biol.* **1997**, *267*, 1002.
- Vijayakumar, M.; Wong, K. Y.; Schreiber, G.; Fersht, A. R.; Szabo, A.; Zhou, H.-X. *J. Mol. Biol.* **1998**, *278*, 1015.
- Born, M. Z. *Phys.* **1920**, *1*, 45.
- Kirkwood, J. G. *J. Chem. Phys.* **1934**, *2*, 351.
- When the ions get exposed to the solvent (i.e., $r > R - a$), eq 2 is not applicable anymore. We calculated the electrostatic energy for such a situation numerically by the UHBD program.¹¹ The UHBD results for buried ions (with $r < R - a$) were indistinguishable from those given by eq 2.
- Ernst, J. A.; Clubb, R. T.; Zhou, H.-X.; Gronenborn, A. M.; Clore, G. M. *Science* **1995**, *267*, 1813.
- Serrano, L.; Horovitz, A.; Avron, B.; Bycroft, M.; Fersht, A. R. *Biochemistry* **1990**, *29*, 9343.
- Buckle, A. M.; Henrick, K.; Fersht, A. R. *J. Mol. Biol.* **1993**, *234*, 847.
- Weiner, S. J.; Kollman, P. A.; Case, D. A.; Singh, U. C.; Ghio, C.; Alagona, G.; Prefeta, S.; Weiner, P. *J. Am. Chem. Soc.* **1984**, *106*, 765.
- It is very possible that, in the unfolded state, the residue to be mutated may not be as exposed as is modeled and that there may be residual interactions between the residue and the rest of the protein. In the absence of additional information, we assume that the opposing effects cancel. However, note the example in the next paragraph in which a specific interaction is included in the unfolded state.
- Oliveberg, M.; Arcus, V. L.; Fersht, A. R. *Biochemistry* **1995**, *34*, 9424.
- Jorgenson, W. L.; Tirado-Rives, J. *J. Am. Chem. Soc.* **1988**, *110*, 1657.
- Brooks, B. R.; Brucoleri, R. E.; Olafson, B. D.; States, D. J.; Swaminathan, S.; Karplus, M. *J. Comput. Chem.* **1983**, *4*, 187.
- Pascual-Ahuir, J. L.; Silla, E.; Tunon, I. *J. Comput. Chem.* **1994**, *15*, 1127.
- Waldburger, C. D.; Schildbach, J. F.; Sauer, R. T. *Nat. Struct. Biol.* **1995**, *2*, 122.
- Antosiewicz, J.; McCammon, J. A.; Gilson, M. K. *J. Mol. Biol.* **1994**, *238*, 415.
- Havranek, J. J.; Harbury, P. B. *Proc. Natl. Acad. Sci. U.S.A.* **1999**, *96*, 11145.
- Hummer, G.; Pratt, L. R.; Garcia, A. E. *J. Phys. Chem.* **1996**, *100*, 1206.
- Wimley, W. C.; Gawrisch, K.; Creamer, T. P.; White, S. H. *Proc. Natl. Acad. Sci. U.S.A.* **1996**, *93*, 2985.
- Luo, R.; David, L.; Hung, H.; Devaney, J.; Gilson, M. K. *J. Phys. Chem. B* **1999**, *103*, 727.